Dependence of Structural Forces in Polyelectrolyte Solutions on Charge Density: A Combined AFM/SAXS Study

Dan Qu,[†] Damien Baigl,[‡] Claudine E. Williams,[‡] Helmuth Möhwald,[†] and Andreas Fery*,[†]

Max Planck Institut für Kolloid- und Grenzflächenforschung, Golm, and Laboratory of Organized Fluids, CNRS UMR 7125, Collège de France, 75005 Paris, France

Received March 11, 2003; Revised Manuscript Received June 27, 2003

ABSTRACT: We have investigated the structural forces in aqueous, salt-free, semidilute solutions of partially sulfonated polystyrene (PSS) of various charge fractions f using colloidal probe atomic force microscopy and small-angle X-ray scattering (SAXS). Near interfaces, we find an exponentially damped oscillatory force−distance characteristic whose period d corresponds to the characteristic length of the density fluctuations in bulk. d scales with monomer concentration C as $d = d_0C^{\alpha}$, where α varies progressively from −0.51 for fully charged PSS to −0.31 for the lowest charge fraction investigated. This can be explained by changes in the polyelectrolyte configuration as the charge is reduced, due to the hydrophobic nature of the backbone. The decay length λ of the force is in all cases proportional to $C^{-1/2}$ and is closely matching the range of positional correlations extracted from the SAXS data. The amplitude A of the force is proportional to the effective charge (f_{eff}) of the polyelectrolyte.

Introduction

Polyelectrolytes are polymeric molecules that can be ionized in water. A vast number of both biological macromolecules such as DNA and most proteins and synthetic macromolecules belong to this category. Classical applications for polyelectrolytes include flocculation agents in wastewater treatment and paper making. In recent years, polyelectrolytes are also increasingly used for coating of paper and textiles or for biocompatible coatings of contact lenses and organ implants. The growing interest in polyelectrolytes for applications is triggered by environmental reasons, as water-based processes are environmentally less harmful than those using organic solvents. In general, even strongly hydrophobic polymers can be made water-soluble by adding ionizable groups. Thus, switching neutral molecules to polyelectrolytes is one of the main strategies to replace organic solvents by water.

At the same time, from a scientific point of view, polyelectrolytes are far less well understood than noncharged polymers because the long-range nature of the electrostatic interactions and the large entropic contribution of the counterions complicate the analysis.[1,2] Specifically, it has been shown theoretically[3−7] and experimentally[8−16] that polyelectrolyte solutions show complex ordering phenomena, as they can form meshlike structures if their concentration is sufficiently high. Indeed for dilute solutions, in which individual molecules do not overlap, the correlation length ξ of the monomer density is given by the average distance between the molecules which is proportional to $C^{-1/3}$, where C is the monomer concentration.[1] This scaling behavior is the same as that found for charged colloidal particles, e.g., in micellar systems.[17,18] However, as the concentration is reaching a critical value, the individual molecules start to overlap, and the solution enters the semidilute regime in which the molecules form a transient meshlike structure. De Gennes et al.[3] predicted a change of the scaling of ξ from $C^{-1/3}$ to $C^{-1/2}$ for this regime. Furthermore, ξ no longer depends on the degree of polymerization of the individual molecules. Indeed, several groups have found, using small-angle X-ray scattering (SAXS) and small-angle neutron scattering (SANS) techniques, that the correlation length associated with the peak in the structure factor in semidilute solutions of various polyelectrolytes ξ scales as $C^{-1/2}$ and is independent of molecular weight over a wide range.[19−22] Independent from these structural studies, several groups investigating polyelectrolytes in confined geometry found oscillatory force−distance characteristics for thin films of semidilute polyelectrolyte solutions.[8−16] Asnacios and co-workers were the first to link the appearance of these oscillatory forces to the bulk mesh structure of polyelectrolyte solutions.[12] Subsequently, several studies have combined scattering spectroscopy/force techniques and confirmed the match of force oscillation period and the length corresponding to the peak in the structure factor.[14−16] Klitzing and coworkers also studied the effect of charge fraction on the structure of semidilute solutions of polyelectrolytes with hydrophilic backbones, where the force period changes with the charge fraction, but the $\xi \sim C^{-1/2}$ power law scaling does not change.[14,15] However, the detailed interactions in solutions, including the force−amplitude and force−decay length, have never been studied experimentally. If the structure of semidilute solutions of highly charged, hydrophilic polyelectrolytes is fairly well understood today, the situation is more complex for semidilute solutions of hydrophobic polyelectrolytes, i.e., when water is a poor solvent for the backbone. While hydrophilic polyelectrolytes are usually adopting a stretched rodlike configuration because of the intramolecular electrostatic repulsion, the configuration of hydrophobic polyelectrolytes is the result of a competition between electrostatic interactions that favor

[†] Max Planck Institut für Kolloid- und Grenzflächenforschung, Golm.
[‡] Laboratory of Organized Fluids, CNRS UMR 7125, Collège de France.
* Corresponding author: e-mail andreas.fery@mpikg-golm.mpg.de.

10.1021/ma034305k CCC: $25.00
Published on Web 08/06/2003

a stretched configuration and hydrophobic interactions that favor a collapsed configuration.[5] Therefore, the scaling behavior is predicted to be more complicated and to depend on the relative strength of the two interactions.[23,24] Indeed, Essafi et al. found that for partially sulfonated polystyrene the power law scaling deviates from the predicted $C^{-1/2}$ for degrees of sulfonation lower than 100%.[25] Recently, Baigl et al. performed a more detailed SAXS study on the effect of charge percentage on the concentration dependency of the structure factor for partially charged PSS.[26,27] On the other hand, using the thin film balance technique, Théodoly and coworkers reported oscillatory force characteristic for these polyelectrolytes, but in the case of PSS, serious complications arose from the instability caused by the slow adsorption of partially sulfonated polystyrene adsorbing at the air−liquid interface of the free-standing film.[28,29]

We have investigated the same system, i.e., salt-free solutions of partially sulfonated PSS in the semidilute regime, using colloidal probe AFM. Using this technique, which was first introduced in this field by Milling and co-workers,[8−10] we can not only circumvent the film stability problems encountered in the thin films studies but also, in contrast to the thin film balance technique that is limited to regions of positive surface pressure, we are able to probe regions of negative surface pressure and thus obtain data on the entire force−distance characteristics. Thus, we have been able to not only obtain information on the oscillation period but also extract information on the interaction within the solution, which is reflected in the oscillation amplitude and decay length. We can further obtain the stiffness of the structure from the derivatives of these force−distance curves. Finally, we have carried out parallel SAXS measurements on the solutions in order to correlate the structural forces to the bulk structure.

Experiments

We have used well-defined monodispersed ($M_W/M_N < 1.3$) same PSS (poly(styrene-*co*-styrenesulfonate, sodium salt) of one same chain length ($N = 410$) and four different charge fractions ranging from 39% to 91%, as model partially charged hydrophobic polyelectrolytes. As fully charged hydrophobic polyelectrolyte, we have used PSS purchased from Aldrich (product number 24,305-1, average molecular weight 70 000, i.e. $N = 340$) and extensively dialized (Spectrapor dialysis membrane MWCO 10 000) against ultraclean water. The partially charged PSS were synthesized and characterized as described in ref 26. All PSS solutions were prepared by weight using ultraclean water (resistivity 18.2 MΩ/cm) without added salt, and the pH values for the solutions are all around 7.

Force−distance measurements were carried out using a commercial atomic force microscope (Molecular Force Probe, Asylum Research). The AFM was equipped with an inductive sensor (LVDT sensor) that measures the piezo extension independently to eliminate artifacts due to piezo creep and hysteresis. We used the colloidal probe technique introduced by Ducker et al.[30] in which the usual sharp AFM tip is replaced by a colloidal particle of known dimensions and glued to a tipless cantilever. Thus, the general energy−distance relation can be inferred from the measured force−separation data using the Derjaguin approximation: $F(x)/2\pi R = E(x)$, where F is the measured force between the bead of radius R and the planar surface and E the interaction energy per area between two planar surfaces with identical interactions at separation x. The Derjaguin approximation is valid under the condition that the maximum range of the force, x_{max}, is much smaller than the bead radius R, which was our case. Tipless cantilevers were obtained from MikroMasch (Ultrasharp Contact Silicon Cantilevers, CSC12), and individual silica particles of diameter ∼7 μm (produced by Bangs Laboratories, Inc.) were glued to the cantilevers with epoxy glue (UHU 2-Komponenten Epoxidharz-kleber, endfest) with the help of a micromanipulator. Sensitivities were determined from the slope in the constant compliant region of the force−distance data, and the spring constant of the cantilevers was measured using the thermal noise method.[31,32] Silicon wafers (Wacker, Germany) were used as substrates and cleaned by an RCA method,[33] stored under water for not longer than 2 days, and blown dry with nitrogen before measurements. Particles glued to the cantilevers were cleaned directly before measurement with plasma cleaning for 20 min (plasma cleaner PDC-32G, Harrick Scientific). Then a drop of PSS solution was put onto the substrate, and the probing head (the silica particle) was immersed into the solution. Force−distance curves were obtained at a pulling frequency of 0.2 Hz, corresponding to a piezo speed between 200 and 800 nm/s, depending on the pulling distance. Within this range of pulling speeds, no dependency of the force curves on the speed was found except for the highest concentration used. In this case, the baselines of approaching and retracting curves were slightly offset due to viscous forces. For each solution, typically 30−50 force−distance curves were measured at 3−5 different locations on the same substrate as well as on 2−4 different substrates. Since the PSS chains have the same charge as the Si/SiO_2 surfaces and the solutions are without additional salt, adsorption of the PSS chains to the surface is unlikely, which is proved by the data, where no adhesion was ever observed.

SAXS measurements were performed in PSS solutions at European Synchrotron Radiation Facility (ESRF, Grenoble, France) on a BM26 beamline. A highly monochromatic ($\Delta\lambda/\lambda \sim 2 \times 10^{-4}$) X-ray beam at $\lambda = 0.124$ nm (10.0 keV) was used. The detector was a 1D quadrant gas-filled detector situated at 7.8 m from the sample. The scattering vectors q ($q = 4\pi/\lambda \sin(\theta/2)$, θ is the scattering angle) ranged from 0.1 to 0.9 nm^{-1}. Standard data treatment was used, and the scattering profiles are presented as intensities in relative units vs q.

Results and Discussion

As opposed to the thin film balance technique that can explore only regions of positive surface pressure, both the positive and negative surface pressure regions are accessible in AFM measurements, thus complete oscillatory force−distance curves could be recorded. Both the amplitude and period of the oscillation change with the percentage of charge and the monomer concentration. Figure 1 shows a series of representative force−distance curves, in which Figure 1a shows the effect of different charge percentages at a fixed monomer concentration ($C = 0.05$ M), and Figure 1b shows the effect of monomer concentration at the same charge percentage ($f = 56\%$).

We can see that, as a general trend, the oscillation becomes weaker when C or f decreases. All these force−distance curves include both the approaching and retracting curves. The jumps in the incomplete curves when C and f are relatively high are due to the fact that the slope of the curves exceeded the spring constant of the cantilever in those cases, which lead to mechanical instability in those regions of the force curves.

To quantitatively and systematically study the influence of the charge percentage f and monomer concentration C on the oscillatory force, we have fitted each individual force−distance curve to the functional form $F/2\pi R = Ae^{-x/\lambda}\cos[2\pi(x/d) + \varphi]$, where F is the force, R is the radius of the colloidal probe, and x is the distance; the four fitting parameters are the oscillation amplitude A, the decay length λ, the oscillation period d, and φ. Such a functional form consisting of a harmonic oscillation coupled with an exponential decay is typical of

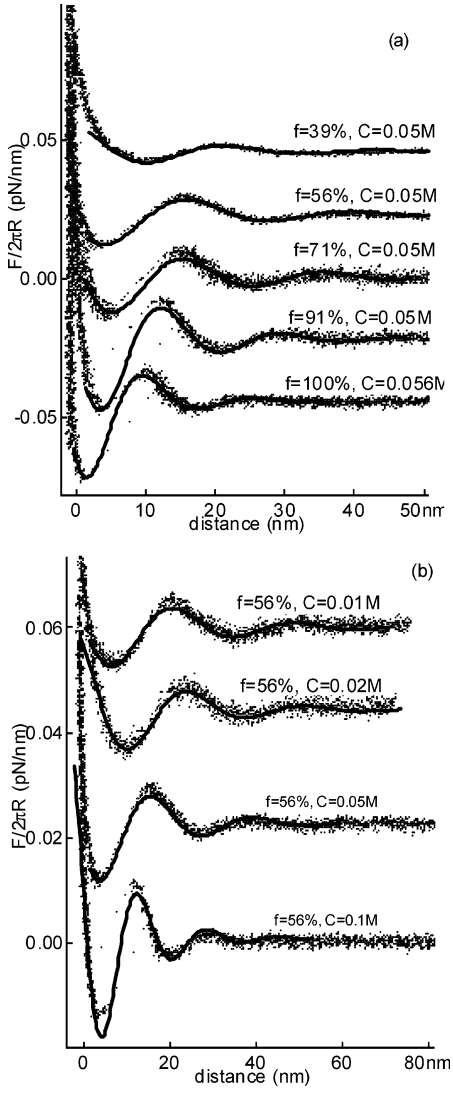

Figure 1. AFM force vs distance curves for PSS (a) of different charge percentages at the same concentration $C = 0.05$ M and (b) of different monomer concentrations at the same charge percentage $f = 56\%$. For better viewing, the curves are offset.

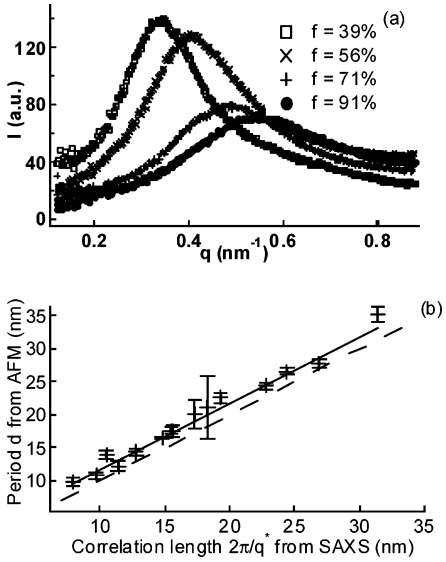

Figure 2. (a) SAXS intensity (arbitrary units) as a function of the wavevector q for differently charged PSS at $C = 0.1$ M. (b) Comparison between the results on the oscillation period d from AFM measurements and the correlation length $2\pi/q^*$ from SAXS measurements for all concentrations and all charge fractions. Cross: data; solid line: linear fit of the data $d = (1.74 \pm 0.41) + (1.00 \pm 0.03)2\pi/q^*$; dashed line: reference line $y = x$.

structural forces that arise when objects of size d are confined between two flat surfaces.[34] In our system, the typical size d is given by the correlation length of the density in the bulk solution, as will be demonstrated below. The amplitude of this density fluctuation increases due to the confinement which gives rise to the structural force. In fitting the force data, we have neglected the region close to hard contact, since additional nonstructural forces are contributing here. The decay length λ is a measure of how well the periodic structure persists within the solution. It is influenced by the properties of the bulk solution and not the presence of the walls, as will be discussed later. The amplitude A measures the strength of the interaction. Thus, the three fit parameters, d, λ, and A, fully describe the force and structure in the solution near interfaces. Each parameter is an average of 10−20 fits to force curves that were randomly selected from the measured force curves.

Dependency of the Force Period on Concentration and Charge Fraction. If the oscillatory force detected here is indeed a structural force, the oscillation period should be identical to the period of the bulk density fluctuations that is measured by SAXS. Thus, the comparison of the force oscillation period to the correlation length $2\pi/q^*$ found in the SAXS measurements is an important first test. Figure 2a presents a representative set of SAXS intensity profiles $I(q)$ at concentration $C = 0.1$ M for differently charged PSS where one can see the broad, characteristic peak at q^* in the case of salt-free solution of polyelectrolytes. Figure 2b shows the comparison between the period d from the AFM measurements and the correlation length $2\pi/q^*$ from the SAXS measurements.

Within experimental uncertainties, we found a good agreement between the two, which supports the explanation of the observed forces as structural forces.

Figure 3a shows the change of the force oscillation period d with the monomer concentration C.

The data for each fixed charge percentage can be fitted to a power law of the form $d = d_0 C^{-\alpha}$. All the α's from the fits are listed in Table 1.

The power α decreases as f decreases, from 0.51 for fully charged PSS chains to 0.31 for the least charged PSS chains. Also, as shown in Figure 3b, the oscillation period is decreasing with the effective charge fraction f_{eff} for all concentrations investigated. We have used the effective charge fraction f_{eff} instead of the chemical charge fraction f for the reason immediately following.

The values of f_{eff} have been taken from osmotic pressure measurements of Essafi et al.[25] In Table 2, the effective charge percentage f_{eff} of the PSS (using the osmotic pressure data of Essafi) is listed as a function of the chemical charge percentage f.

These measured values of values of f_{eff} show that, for PSS, the effective charge of a single chain deviates strongly from the predictions of Manning−Oosawa theory (MO theory).[35,36] It is predicted that for rodlike (extended), highly charged polyelectrolytes a proportion of counterions remain bound to the chain in such a way that the effective charge is renormalized to a constant value whenever the average distance between ionizable

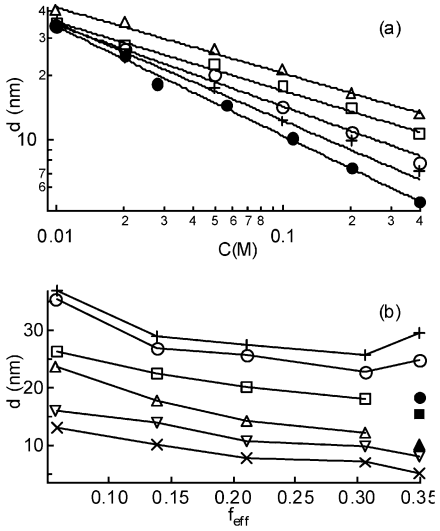

Figure 3. (a) Force oscillation period d vs monomer concentration C for differently charged PSS. Closed circle: $f = 100\%$; cross: $f = 91\%$; open circle: $f = 71\%$; open square: $f = 56\%$; open triangle: $f = 39\%$; solid lines: fits to $d = d_0C^{-\alpha}$. (b) d vs effective charge percentage f_{eff} at different monomer concentrations. Cross: $C = 0.01$ M; open circle: $C = 0.02$ M; closed circle: $C = 0.028$ M; open square: $C = 0.05$ M; closed square: $C = 0.056$ M; open triangle: $C = 0.1$ M; closed triangle: $C = 0.111$ M; inverted open triangle: $C = 0.2$ M; tilted cross: $C = 0.4$ M. Symbols representing the same concentration are connected by solid lines to guide the eyes.

Table 1. Results for α and β from the Fits of $d = d_0C^{-\alpha}$ and $\lambda = \lambda_0C^{-\beta}$

f	100%	91%	71%	56%	39%
α	0.51 ± 0.02	0.46 ± 0.01	0.38 ± 0.01	0.32 ± 0.01	0.31 ± 0.01
β	0.54 ± 0.02	0.53 ± 0.09	0.50 ± 0.10	0.50 ± 0.03	0.52 ± 0.08

Table 2. Chemical Charge Percentage f and Effective Charge Percentage f_{eff} for the PSS Samples

f	39%	56%	71%	91%	100%
f_{eff}	5.8%	14%	21%	31%	35%

groups along the chain is the same as the Bjerrum length ($l_B = 7.1$ Å at 25 °C in water, $l_B = 4\pi\epsilon k_BT/e^2$, where T is the temperature, k_B is the Boltzmann constant, and ϵ is the dielectric constant). Indeed, such behavior has been found for several polyelectrolytes with hydrophilic backbone.[15,16] However, for PSS which has a hydrophobic backbone, the strong reduction of f_{eff} together with a large body of experimental data on PSS using various techniques has shown that hydrophobic interactions influence profoundly the chain conformation.[37−39] To understand the chain conformation, let us first look at whether the chains overlap with each other. It is thus important to know the influence of the chain length on the characteristic length, since the characteristic length should not depend on the chain length if the chains are entangled and should depend on the chain length if the chains do not overlap. Previous SAXS data have shown that for charges above 50% there is no influence of chain length on the characteristic length.[26] This indicates that for $f > 50\%$ the solutions are in the semidilute regime, and the chains entangle with each other to form transient structures. However, recent data on PSS samples of $f < 50\%$ indicate a tendency of increased characteristic length with chain length (SAXS data not shown here since it is still preliminary). This could mean that the solutions are in the dilute regime and the chains keep their individuality, which explains the $-1/3$ exponent.[1] Because of the solubility limit, we are not able to increase the concentration for the lowest charged PSS any further.

For $f > 50\%$, the findings are compatible with the pearl necklace model, first introduced by Dobrynin and Rubinstein,[23,24] based on the scaling concepts and later confirmed by more elaborate theoretical calculations and simulations.[40−42] (It is important to note that the model of an elongated cylinder for a polyelectrolyte in poor solvent, first introduced by Khokhlov,[5] does not agree with the experimental findings for PSS, since all our PSS solutions are homogeneous and do not form gels.) In light of the pearl necklace model, we see the chain configuration as the result of a competition between a hydrophobic effect that causes the chains to collapse into dense globules and an electrostatic effect that restricts the maximum size of the globule. Since charged droplets become unstable when the energy of electrostatic repulsion is reaching the same magnitude as the interfacial energy, a molecule does not collapse into one globule but forms several globules (pearls) that are connected by strings (necklace). This pearl necklace configuration can indeed lead to a change in the scaling behavior. Qualitatively, there are two semidilute regimes. If the correlation length is large as compared to both the pearl size and the distance between the pearls, the scaling should be the same as for a hydrophilic polyelectrolyte solution. But as soon as the correlation length becomes comparable to the separation of the pearls, the structure will be like a densely packed solution of beads and no longer like a mesh. Thus, with increasing concentration, the scaling should change from $d \sim C^{-1/2}$ to $d \sim C^{-1/3}$, the latter typical for dilute solutions or solutions of isolated, centrosymmetric objects.[17,18,43,44] In addtion to the pearl necklace model, Schiessel[45] has given a compatible scaling picture for flexible polyelectrolytes with counterion condensation and pointed out that PSS chains will gradually collapse as the charge fraction decreases and the hydrophobicity increases and that the scaling should change gradually from $C^{-1/2}$ to $C^{-1/3}$. Recently, Limbach et al. have performed molecular dynamics simulations on polyelectrolytes in poor solvent conditions. At $f = 50\%$, they have found that the position of the first peak q^* in the structure factor scaled as $C^{0.35}$. The 0.35 exponent is close to the value of α we have found at $f = 56\%$ (see Table 1).

Dependency of the Decay Length and Amplitude on Solution Conditions. The decay length λ and the amplitude A are measures of the range and strength of the structural forces. In parts a and b of Figure 4, the decay length λ is plotted as a function of C and f_{eff}, respectively.

Although the data are more scattered than those of the oscillation period, the decrease of λ with both C and f_{eff} can be clearly identified. A fit of λ vs C to the form $\lambda = \lambda_0C^{-\beta}$ shows that the scaling of λ is independent of the effective charge fraction, other than in the case of the oscillation period. The fitted results for β's are listed in Table 1. For all effective charge densities, a scaling coefficient of $-1/2$ is found, which reminds us of the scaling of the counterion screening which is described by the Debye−Hückel length $\lambda_{DH} = 1/\sqrt{4\pi l_B f_{eff} C}$. Indeed, as shown in Figure 5, we find that λ is equal to the Debye−Hückel length for the lowest charge fraction.

This indicates that, at this charge fraction, the interaction is dominated by counterion screening. When the charge fraction increases, we find that the decay

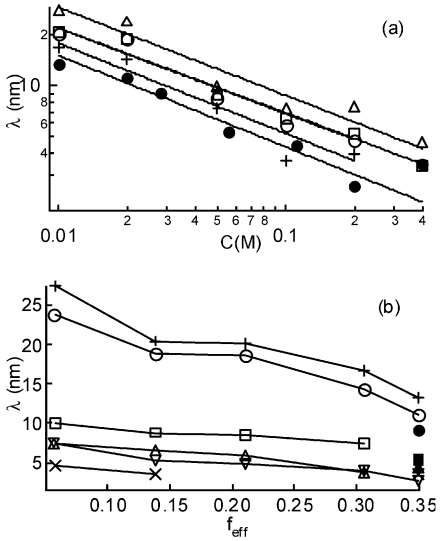

Figure 4. (a) Force decay length λ vs monomer concentration C for differently charged PSS. Closed circle: $f = 100\%$; cross: $f = 91\%$; open circle: $f = 71\%$; open square: $f = 56\%$; open triangle: $f = 39\%$; solid lines: fits to $\lambda = \lambda_0 C^{-\beta}$. (b) λ vs f_{eff} at different monomer concentrations. Cross: $C = 0.01$ M; open circle: $C = 0.02$ M; closed circle: $C = 0.028$ M; open square: $C = 0.05$ M; closed square: $C = 0.056$ M; open triangle: $C = 0.1$ M; closed triangle: $C = 0.111$ M; inverted open triangle: $C = 0.2$ M; tilted cross: $C = 0.4$ M. Symbols representing the same concentration are connected by solid lines to guide the eyes.

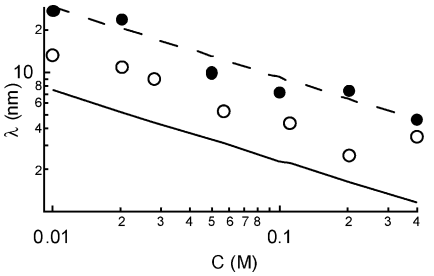

Figure 5. Comparison between the force decay length λ from the AFM measurements and the calculated Debye−Hückel length λ_{DH}, both vs C, for two different charge fractions. Open circle: λ for $f = 100\%$ ($f_{\text{eff}} = 35\%$); closed circle: λ for $f = 39\%$ ($f_{\text{eff}} = 5.8\%$); solid line: λ_{DH} for $f = 100\%$ ($f_{\text{eff}} = 35\%$); dotted line: λ_{DH} for $f = 39\%$ ($f_{\text{eff}} = 5.8\%$).

length is getting systematically larger than λ_{DH} until it reaches about twice the value of the Debye−Hückel length for the fully sulfonated polystyrene. This deviation of λ from λ_{DH} at high charge fractions could be explained by additional influences of the monomer−monomer interactions on the free energy of the system and, consequently, the decay length.[1,2,46]

Since the periodical structure is itself a bulk property, the force decay should not indicate the disappearance of the oscillation. From above, we have also seen that the decay length indeed depends on C and f_{eff}, both bulk properties. To further understand λ, we relate it to the width of the peaks in the SAXS experiments (examples of which are shown in Figure 2a). The SAXS peak width at half-maximum Δq is purely a bulk property and indicates the correlation range χ of the positional order. For exponentially decaying positional correlations, $\chi = 2/\Delta q$.[47] We have seen from Figure 2a that Δq is clearly getting wider as the charge increases. In Figure 6, we have plotted χ vs our decay length λ at $C = 0.1$ M for different charges ($f = 91\%$, 71%, 56%, and 39%).

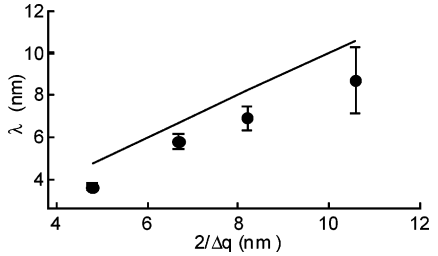

Figure 6. Comparison between AFM decay length λ and the positional correlation range in bulk $2/\Delta q$ measured from the SAXS peak width. Closed circle: data; solid line: theoretical prediction for the decay length and the range of positional correlation if the decay is exponential: $\lambda = 2/\Delta q$.

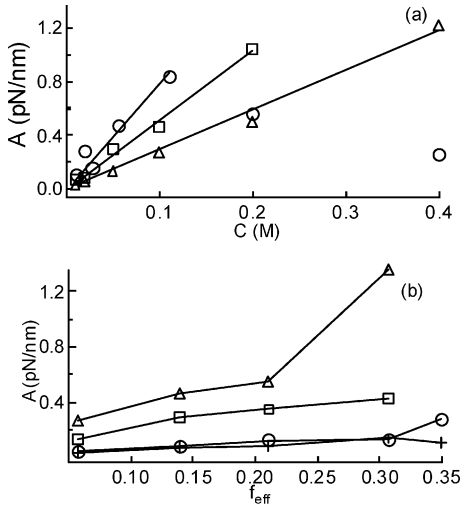

Figure 7. (a) Oscillation amplitude A vs C for three different charge percentages. Open circle: $f = 100\%$; open square: $f = 56\%$; open triangle: $f = 39\%$; solid lines: linear fits to $A = A_0 C$. (The last two data points for $f = 100\%$ are excluded from the fit.) (b) A vs f_{eff} for four different monomer concentrations. Cross: $C = 0.01$ M; open circle: $C = 0.02$ M; open square: $C = 0.05$ M; open triangle: $C = 0.1$ M. Symbols representing the same concentration are connected by solid lines to guide the eyes.

We find that $\chi \sim \lambda$ within the experimental errors, which suggests that the force decay is indeed exponential and mainly caused by the loss of positional correlations.

To better understand the interaction strength, the oscillation amplitude A is plotted as a function of C and f_{eff} respectively in parts a and b of Figure 7.

For clear viewing, only three representative charge percentages are shown in Figure 7a. We see that A increases with both C and f_{eff}. For the two highest charge percentages, namely $f = 91\%$ (not shown in Figure 7a) and $f = 100\%$ (as shown in Figure 7a), the amplitude decreases when the concentration is above 0.1 M. A similar behavior has also been found by others;[8,9] it can be possibly explained by the fact that at these high concentrations the solution is no longer in the semidilute regime but in a concentrated regime. Another possible reason could be the increasing viscosity of the solution that perturbs the measurement. However, within the range where A increases with C, A depends linearly on C. Linear fits to $A = A_0 C$ are also shown in Figure 7a. The slope A_0 of the fits increases as f increases. This is compatible with the assumption that the main contribution of the structural force stems from the osmotic pressure of the counterions whose density is linear in the polyelectrolyte concentration and

in the effective charge fraction. This close to linear increase of A with f_{eff} is confirmed again in Figure 7b. Therefore, the higher the charge fraction is, the stronger the corresponding structural force becomes.

Since the slope of the force−distance curve reflects the stiffness of the structure, we can easily understand the change of the stiffness with C and f by taking the derivative of $F/2\pi R$:

$$\frac{1}{2\pi R}\frac{\mathrm{d}F}{\mathrm{d}x} = A\sqrt{\left(\frac{1}{\lambda}\right)^2 + \left(\frac{2\pi}{d}\right)^2}\,\mathrm{e}^{-x/\lambda}\cos\left(2\pi\frac{x}{d} + \varphi'\right),$$

$$\text{where } \varphi - \varphi' = \tan^{-1}\left(\frac{2\pi\lambda}{d}\right)$$

The coefficient $A/\sqrt{(1/\lambda)^2+(2\pi/d)^2}$ thus controls the stiffness, on which all three parameters, A, d, and λ have their effects. When C and f increase, both d and λ decrease and A increases; thus, $A/\sqrt{(1/\lambda)^2+(2\pi/d)^2}$ increases and the polyelectrolyte structure is stiffer. This is independent of the chain configuration.

Conclusions

We have studied the forces and structures of fully and partially charged PSS solutions in the semidilute regime and investigated the effect of hydrophobicity, effective charge percentage, and monomer concentration on the structures and interactions in the solutions. AFM as our main technique has provided us direct and detailed structural information in real space. SAXS as a complementary technique has enabled us to extract information in reciprocal space about bulk solution only and helped us to understand whether the phenomena were due to effects of the surfaces. We have fitted the force−distance curves to a harmonic oscillation coupled with exponential decay and, for the first time, extracted quantitative information not only on the period but also on the amplitude and the decay length. We have found progressive power law dependencies of the period on the monomer concentration in the form of $d \sim C^{-\alpha}$, with α changing from $^1/_2$ to $^1/_3$ as the charge percentage decreases. This indicates a change of the chain configuration in the semidilute regime with the effective charge. We have further found that the decay length of the oscillatory force is equal to the range of positional correlations extracted from the SAXS peak width, which suggests that the force decay is indeed mainly caused by the loss of positional correlations. The decay length of all these PSS solutions of different charge percentages scales with $-^1/_2$ power of the monomer concentration, similar to that predicted by Debye−Hückel theory, but with a different prefactor. The difference between the two decreases as the effective charge decreases. The decay length finally reduces to the Debye−Hückel length at the effective charge percentage of 5.8%. This indicates that the decay length is determined by the electrostatic interactions in the solution rather than by the conformational properties at this lowest charge fraction, while at higher charges, there exists the influence of monomer−monomer interactions. The oscillation amplitude increases with both the concentration and the charge fraction, which is compatible with the assumption that the structural force is mainly caused by the osmotic pressure of the counterions. Consequently, the stiffness of the structure increases with both the concentration and the charge percentage.

Acknowledgment. We thank Regine von Klitzing for valuable discussions. This work is supported by the Max-Planck Society and by the DFG within the German/French collaboration research group "Complex Fluids: from 3D to 2D".

References and Notes

(1) Barrat, J.-L.; Joanny, J.-F. *Adv. Chem. Phys.* **1996**, *94*, 1.
(2) Netz, R. R.; Andelman, D. *Phys. Rep.* **2003**, *380*, 1.
(3) De Gennes, P.-G.; Pincus, P.; Velasco, R. M.; Brochard, F. *J. Phys. (Paris)* **1976**, *37*, 1461.
(4) Odijk, T. *J. Polym. Sci., Polym. Phys.* **1977**, *15*, 477.
(5) Khokhlov, A. R.; Khachaturian, K. A. *Polymer* **1982**, *23*, 1742.
(6) Dobrynin, A. V.; Colby, R. H.; Rubinstein, M. *Macromolecules* **1995**, *28*, 1859.
(7) Châtellier, X.; Joanny, J.-F. *J. Phys. II* **1996**, *6*, 1669.
(8) Milling, A. J. *J. Phys. Chem.* **1996**, *100*, 8986.
(9) Kendall, K.; Milling, A. J. *Langmuir* **2000**, *16*, 5106.
(10) Milling, A. J.; Vincent, B. *J. Chem. Soc., Faraday Trans.* **1997**, *93*, 3179.
(11) Bergeron, V.; Langevin, D.; Asnacios, A. *Langmuir* **1996**, *12*, 1550.
(12) Asnacios, A.; Espert, A.; Colin, A.; Langevin, D. *Phys. Rev. Lett.* **1997**, *78*, 4974.
(13) Klitzing, R. v.; Espert, A.; Asnacios, A.; Hellweg, T.; Colin, A.; Langevin, D. *Colloids Surf. A* **1999**, *149*, 131.
(14) Klitzing, R. v.; Espert, A.; Colin, A.; Langevin, D. *Colliods Surf. A* **2001**, *176*, 109.
(15) Kolaríc, B.; Jaeger, W.; Klitzing, R. v. *J. Phys. Chem. B* **2000**, *104*, 5096.
(16) Théodoly, O.; Tan, J. S.; Ober, R.; Williams, C. E.; Bergeron, V. *Langmuir* **2001**, *17*, 4910.
(17) Bergeron, V.; Radke, C. J. *Langmuir* **1992**, *8*, 3020.
(18) Bergeron, V.; Jiménez-Laguana, A. J.; Radke, C. J. *Langmuir* **1992**, *8*, 3927.
(19) Nierlich, M.; Williams, C. E.; et al. *J. Phys. (Paris)* **1979**, *40*, 701.
(20) Nierlich, F.; Boué, F.; Lapp, A.; Oberthür, R. *Colloid Polym. Sci.* **1985**, *263*, 955.
(21) Nierlich, F.; Boué, F.; Lapp, A.; Oberthür, R. *J. Phys. (Paris)* **1985**, *46*, 649.
(22) Förster, S.; Schmidt, M. *Adv. Polym. Sci.* **1995**, *120*, 51.
(23) Dobrynin, A. V.; Rubinstein, M.; Obukhov, S. P. *Macromolecules* **1996**, *29*, 2974.
(24) Dobrynin, A. V.; Rubinstein, M. *Macromolecules* **1999**, *32*, 915.
(25) Essafi, W. Ph.D. Thesis, Paris VI, France, 1996.
(26) Baigl, D.; Ober, R.; Qu, D.; Fery, A.; Williams, C. E. *Europhys. Lett.* **2003**, *62*, 588.
(27) Baigl, D.; Seery, T. A. P.; Williams, C. E. *Macromolecules* **2002**, *35*, 2318.
(28) Théodoly, O.; Ober, R.; Williams, C. E. *Eur. Phys. J. E* **2001**, *5*, 51.
(29) Théodoly, O. Ph.D. Thesis, Paris VI, France, 1999.
(30) Ducker, W. A.; Senden, T. J.; Pashley, R. M. *Nature (London)* **1991**, *353*, 239.
(31) Hutter, J. L.; Bechhoefer, J. *Rev. Sci. Instrum.* **1993**, *64*, 1868.
(32) Butt, H. J.; Jaschke, M. *Nanotechnology* **1995**, *6*, 1.
(33) Riegler, H.; Engel, M. *Ber. Bunsen-Ges. Phys. Chem.* **1991**, *95*, 1424.
(34) Israelachvili, J. *Intermolecular & Surface Forces*; Academic Press Limited: London, Chapter 13, p 260, 1992.
(35) Manning, G. S. *J. Chem. Phys.* **1969**, *51*, 924.
(36) Oosawa, F. *Polyelectrolytes*; Marcel Dekker: New York, 1971.
(37) Holm, C., et al., Eds.; *Electrostatic Effects in Soft Matter and Biophysics*; Kluwer Academic Publishers: Dordrecht, 2001; p 487.
(38) Baigl, D.; Sferrazza, M.; Williams, C. E. *Europhys. Lett.* **2003**, *62*, 110.
(39) Lee, M.-J.; Green, M. M.; Mikeš, F.; Morawetz, H. *Macromolecules* **2002**, *35*, 4216.
(40) Shew, C.-Y.; Yethiraj, A. *J. Chem. Phys.* **1999**, *110*, 676.
(41) Solis, F. J.; De la Cruz, M. O. *Macromolecules* **1998**, *31*, 5502.
(42) Limbach, H. J.; Holm, C.; Kremer, K. *Europhys. Lett.* **2002**, *60*, 566.
(43) Wassan, D. T.; Nikolov, A. D.; Kralchevsky, P. A.; Ivanov, I. B. *Colloids Surf.* **1992**, *67*, 139.
(44) Pollard, M. L.; Radke, C. J. *J. Chem. Phys.* **1994**, *101*, 6979.
(45) Schiessel, H. *Macromolecules* **1999**, *32*, 5673.
(46) Joanny, J.-F.; Leibler, L. *J. Phys. (Paris)* **1990**, *51*, 545.
(47) Helm, C. A.; Möhwald, H.; Kjaer, K.; Als-Nielsen, J. *Biophys. J.* **1987**, *52*, 381−390.

MA034305K